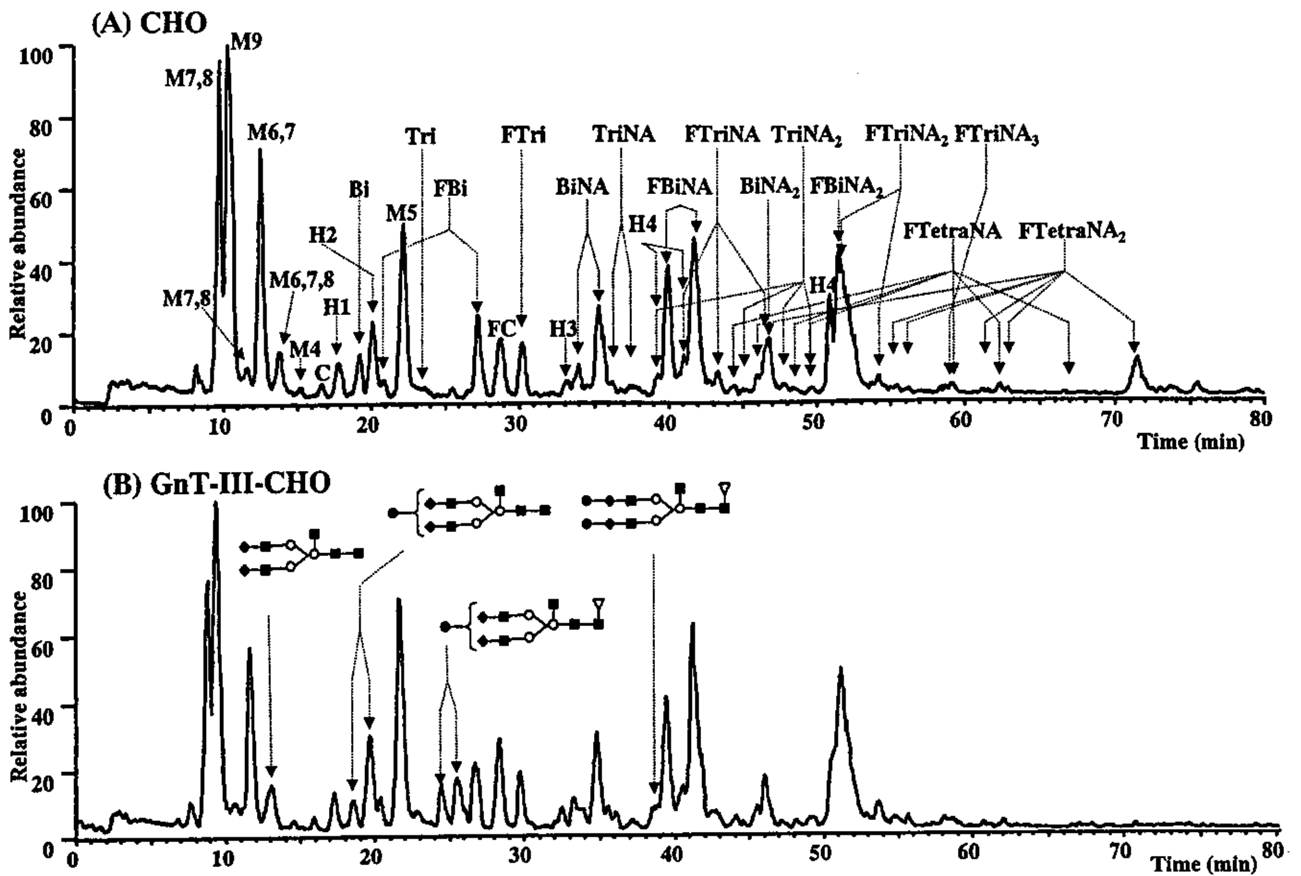

Fig. 3. (A) CHO 細胞膜画分の糖鎖プロファイル，(B) GnT-III 遺伝子導入 CHO 細胞の糖鎖プロファイル

M, Man; H, hybrid; C, trimannosylcore; F, Fuc; NA, NeuAc; Bi, biantennary; Tri, triantennary; Tetra, tetraantennary

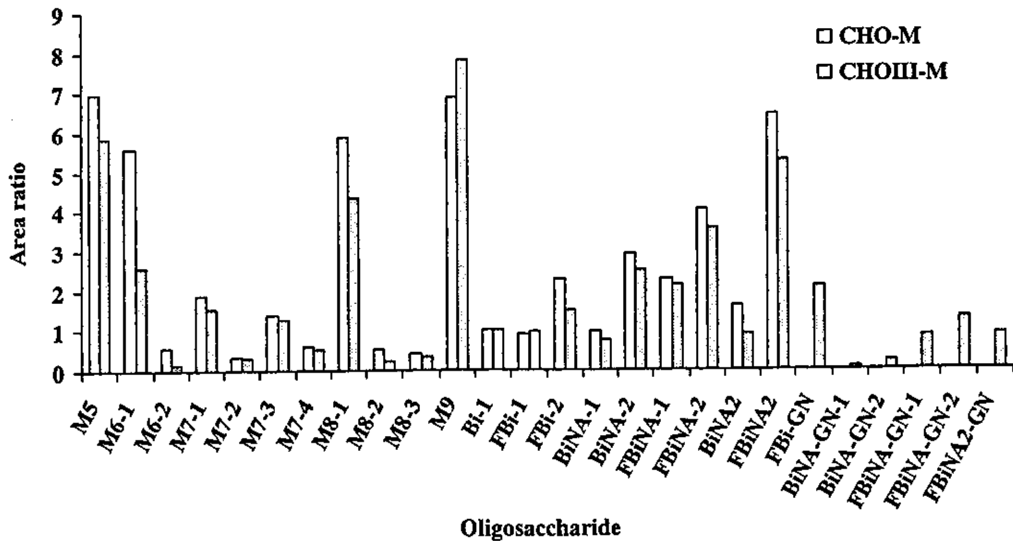

Fig. 4. CHO 細胞膜画分（CHO-M）及び GnT-III 遺伝子導入細胞由来膜画分（CHOIII-M）由来糖鎖の分布

アシアロ 2 本鎖糖鎖を 1.0 とする

2. 糖タンパク質の同定と特性解析

糖鎖差異解析によって疾患関連糖鎖を見出すことができれば，プロテオミクスの手法を用いて，その糖鎖が付加しているタンパク質の同定と特性解析を行うことになる．可溶性タンパク質であれば，レクチンカラムや免疫沈降法などで得られた画分を SDS-PAGE 等で展開して目的糖タンパク質を得ることができるが，不溶性膜タンパク質の場合，レクチン等による分画が難しいケースが多く，2-DE 後，レ

(A) 2D-PAGE

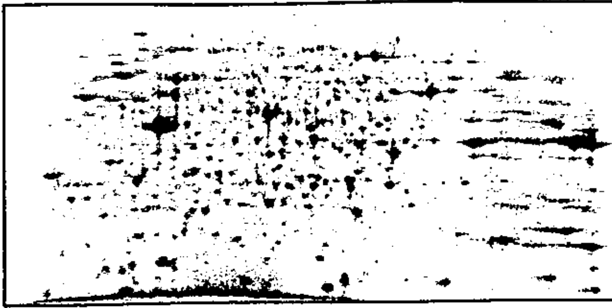

(B) Lectin blot

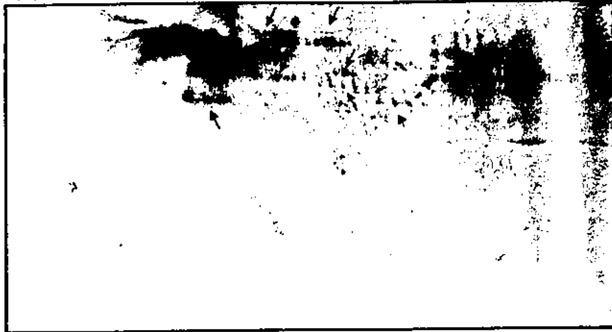

Fig. 5. GnT-III 遺伝子導入細胞膜画分の 2-DE

(A) Sypro Orange 染色, (B) PHA-E_4 ブロット
IEF, pH 3-10, 18 cm, 33,500 Vhr; SDS-PAGE, 12.5% gel (24×11 cm), 20 mA-0.5 hr, 50 mA-1.2 hr

クチンブロットなどにより糖タンパク質の位置を特定することになる[12]. しかし後者の場合, 泳動ゲルとレクチンブロット膜のマッチング, 及び特定されたゲル上タンパク質に目的糖鎖が付加していることの検証が必要となってくる.

Fig. 5 は, GnT-III 遺伝子導入細胞の膜画分を 2 枚のゲルで展開し, Sypro Orange で全タンパク質を染色した結果 (A), 及び bisecting GlcNAc を認識する PHA-E_4 レクチンを用いてレクチンブロットを行った結果 (B) を示している. レクチンブロットによって, 酸性側の 70–80 kDa 周辺に, 糖タンパク質に特徴的な train 状のスポットが複数組検出され, 一部のタンパク質の糖鎖に bisecting GlcNAc が付加されていることが確認された. 我々は, レクチンブロット上のスポットの位置から特定された泳動ゲル上の糖タンパク質の糖鎖の解析にも糖鎖プロファイリングが役立つと考えている. 現在, bisecting GlcNAc が付加していると推定されたスポットについて, ゲル内トリプシン消化に先立ち PNGase F 消化を行って糖鎖を切り出し, GCC-LC/MS を用いた bisecting GlcNAc の有無の確認と糖鎖構造解析を行っているところである.

おわりに

GCC-LC/MS を用いた糖鎖プロファイリングは, 糖タンパク質性医薬品の特性・品質解析を目的として開発されたものである. この糖鎖プロファイリングが, 2-DE 等のプロテオミクス的手法と組み合わせることによって, 医薬品開発型研究のグライコミクスにも応用できる可能性がでてきた. 電気泳動ゲル上の全タンパク質の中から糖タンパク質を検出する方法は報告されているが[13,14], 特定の糖鎖を付加している糖タンパク質のみを検出・抽出する方法は確立されておらず, それらを効率的に検出する方法の確立が今後の課題であろう.

文　献

1) Durand G, Seta N. Protein glycosylation and diseases: blood and urinary oligosaccharides as markers for diagnosis and therapeutic monitoring. Clin Chem 2000;46:795–805.
2) Fenselau C. MALDI MS and strategies for protein analysis. Anal Chem 1997;69:661A–665A.
3) Kawasaki N, Ohta M, Hyuga S, Hashimoto O, Hayakawa T. Analysis of carbohydrate heterogeneity in a glycoprotein using liquid chromatography/mass spectrometry and liquid chromatography with tandem mass spectrometry. Anal Biochem 1999;269:297–303.
4) Itoh S, Kawasaki N, Ohta M, Hyuga M, Hyuga S, Hayakawa T. Simultaneous microanalysis of N-linked oligosaccharides in a glycoprotein using microbore graphitized carbon column liquid chromatography/mass spectrometry. J Chromatogr 2002;168:89–100.
5) Kawasaki N, Itoh S, Ohta M, Hayakawa T. Microanalysis of N-linked oligosaccharides in a glycoprotein by capillary liquid chromatography/mass spectrometry and liquid chromatography/tandem mass spectrometry. Anal Biochem 2003;316:15–22.
6) Baker KN, Rendall MH, Hills AE, Hoare, M, Freedman RB, James DC. Metabolic control of recombinant protein N-glycan processing in NS0 and CHO cells. Biotechnol Bioeng 2001;73:188–202.
7) Sheeley DM, Merrill BM, Taylor LC. Characterization of monoclonal antibody glycosylation: comparison of expression systems and identification of terminal alpha-linked galactose. Anal Biochem 1997;247:102–110.
8) Rudd PM, Colominas C, Royle L, Murphy N, Hart E, Merry, AH, Hebestreit HF, Dwek RA. A high-performance liquid chromatography based strategy for rapid, sensitive sequencing of N-linked oligosaccharide modifications to proteins in sodium dodecyl sulphate polyacrylamide electrophoresis gel bands. Proteomics 2001;1:285–294.
9) Sheng Y, Yoshimura M, Inoue S, Oritani K, Nishiura T, Yoshida H, Ogawa M, Okajima Y, Matsuzawa Y, Taniguchi N. Remodeling of glycoconjugates on CD44 enhances cell adhesion to hyaluronate, tumor growth and metastasis in B16 melanoma cells expressing beta1,4-N-acetylglucosaminyltransferase III. Int J Cancer 1997;73:850–858.
10) Yoshimura M, Nishikawa A, Ihara Y, Taniguchi S, Taniguchi N. Suppression of lung metastasis of B16 mouse melanoma by N-acetylglucosaminyltransferase III gene transfection. Proc Natl Acad Sci USA 1995;92:8754–8758.

11) Yoshimura M, Ihara Y, Matsuzawa Y, Taniguchi N. Aberrant glycosylation of E-cadherin enhances cell-cell binding to suppress metastasis. J Biol Chem 1996;271:13811–13815.
12) Ekuni A, Miyoshi E, Ko JH, Noda K, Kitada T, Ihara S, Endo T, Hino A, Honke K, Taniguchi N. A glycomic approach to hepatic tumors in N-acetylglucosaminyltransferase III (GnT-III) transgenic mice induced by diethylnitrosamine (DEN): identification of haptoglobin as a target molecule of GnT-III. Free Radic Res 2002;36:827–833.
13) Wilson NL, Schulz BL, Karlsson NG, Packer NH. Sequential analysis of N- and O-linked glycosylation of 2D-PAGE separated glycoproteins. J Proteome Res 2002;1:521–529.
14) Schulenberg B, Beechem JM, Patton WF. Mapping glycosylation changes related to cancer using the Multiplexed Proteomics technology: a protein differential display approach. J Chromatogr B Analyt Technol Biomed Life Sci 2003;793:127–139.

Available online at www.sciencedirect.com

SCIENCE @ DIRECT®

Biologicals 32 (2004) 70–77

BIOLOGICALS

www.elsevier.com/locate/biologicals

Analysis of site-specific glycosylation in recombinant human follistatin expressed in Chinese hamster ovary cells

Masashi Hyuga*, Satsuki Itoh, Nana Kawasaki, Miyako Ohta, Akiko Ishii, Sumiko Hyuga, Takao Hayakawa

Division of Biological Chemistry and Biologicals, National Institute of Health Sciences, 1-18-1, Kamiyoga, Setagaya-ku, Tokyo 158-8501, Japan

Received 22 October 2003; accepted 1 April 2004

Abstract

Follistatin (FS), a glycoprotein, plays an important role in cell growth and differentiation through the neutralization of the biological activities of activins. In this study, we analyzed the glycosylation of recombinant human FS (rhFS) produced in Chinese hamster ovary cells. The results of SDS-PAGE and MALDI-TOF MS revealed the presence of both non-glycosylated and glycosylated forms. FS contains two potential *N*-glycosylation sites, Asn95 and Asn259. Using mass spectrometric peptide/glycopeptide mapping and precursor-ion scanning, we found that both *N*-glycosylation sites were partially glycosylated. Monosaccharide composition analyses suggested the linkages of fucosylated bi- and triantennary complex-type oligosaccharides on rhFS. This finding was supported by mass spectrometric oligosaccharide profiling, in which the *m/z* values and elution times of some of the oligosaccharides from rhFS were in good agreement with those of standard oligosaccharides. Site-specific glycosylation was deduced on the basis of the mass spectra of the glycopeptides. It was suggested that biantennary oligosaccharides are major oligosaccharides located at both Asn95 and Asn259, whereas the triantennary structures are present mainly at Asn95.

© 2004 The International Association for Biologicals. Published by Elsevier Ltd. All rights reserved.

Abbreviations: CHO, Chinese hamster ovary; FCS, fetal calf serum; FS, follistatin; GCC, graphitized carbon column; GnT, *N*-acetylglucosaminyltransferase; HPAEC-PAD, high-pH anion-exchange chromatography with pulsed amperometric detection; IEF, isoelectric focusing; LC/MS, liquid chromatography/mass spectrometry; MALDI-TOF MS, matrix-assisted laser desorption/ionization time-of-flight mass spectrometry; NeuAc, *N*-acetyl neuraminic acid; NeuGc, *N*-glucoryl neuraminic acid; PNGaseF, peptide *N*-glycanase F; rhFS, recombinant human follistatin; SDS-PAGE, sodium dodecyl sulfate-polyacrylamide gel electrophoresis; TFA, trifluoroacetic acid

1. Introduction

Follistatin (FS), a glycoprotein, was first discovered in ovarian follicular fluid as an inhibitor of pituitary follicle-stimulating hormone secretion [1,2]. Subsequent studies have revealed that FS can bind to activins and neutralize their biological activities [3,4]. Activins are members of the transforming growth factor-β superfamily, and they play important roles in the regulation of cell growth and in the differentiation processes that lead to morphogenesis in early vertebrate development [5,6]. Since FS and activins are broadly distributed, they are not confined solely to tissues associated with reproduction [7].

FS is present in heterogeneous forms [8]. The FS gene consists of 315 amino acids, and it includes six exons (Fig. 1); alternative splicing can generate two isoforms, i.e. a 315-amino-acid protein (the full-length form, FS315) and a 288-amino-acid protein (the carboxy-truncated form, FS288) [9]. The activin-neutralizing activity of FS288 is higher than that of FS315 [10,11], which appears to correlate with their heparin/heparan sulfate proteoglycan-binding abilities [12]. The heterogeneity of FS is also due to diverse glycosylation. FS has two potential *N*-glycosylation sites (Asn95 and Asn259). Oligosaccharides are generally known to play important roles in defining the properties of glycoproteins such as their biological activity, immunogenicity,

* Corresponding author. Fax: +81-3-3700-9084.
E-mail address: mhyuga@nihs.go.jp (M. Hyuga).

1045-1056/04/$30.00 © 2004 The International Association for Biologicals. Published by Elsevier Ltd. All rights reserved.
doi:10.1016/j.biologicals.2004.04.001

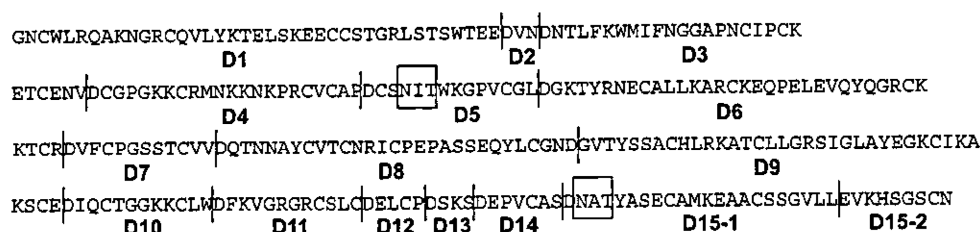

Fig. 1. Amino acid sequence of rhFS. Predicted cleavage sites with Asp-N are indicated by |. The potential *N*-glycosylation sites are indicated by boxes.

pharmacokinetics, solubility, and protease resistance [13,14]. Glycosylation on FS is also likely to exert an effect on activin-neutralizing activity; however, neither structure of the N-linked oligosaccharides in FS, nor their physiological roles, have been clarified due to the limited availability of these oligosaccharides.

The aim of this study was to elucidate the glycosylation of FS. We previously developed an oligosaccharide profiling method using liquid chromatography/mass spectrometry (LC/MS) equipped with a graphitized carbon column (GCC) [15–22]. Recently, we demonstrated a procedure for facilitating the structural analysis of glycoproteins [16]. Carbohydrate profiles and site-specific glycosylations can be characterized by the GCC-LC/MS method, followed by mass spectrometric peptide/glycopeptide mapping. We used this method to demonstrate here the carbohydrate heterogeneity and the site-specific N-linked oligosaccharide structures in recombinant human FS288 (rhFS) produced in Chinese hamster ovary (CHO) cells, in which a sufficient amount of FS could be expressed.

2. Materials and methods

2.1. Materials

Human FS315 cDNA and recombinant human activin A were kindly provided by Dr. Yuzuru Eto (Ajinomoto Co., Inc., Kawasaki, Japan). CHO cells were obtained from the Japanese Cancer Research Resources Bank (Tokyo, Japan). Mammalian expression vector pcDNA3.1/Hygro was purchased from Invitrogen (Carlsbad, CA, USA). LipofectAMINE plus reagent, Ham's F12 medium, fetal calf serum (FCS) and hygromycin were purchased from Life Technologies Inc. (Rockville, MD, USA). Pellicon XL membrane and Immobilon-P membrane were purchased from Millipore Corp. (Bedford, MA, USA). Sulfated-cellulofine was purchased from Seikagaku Corp. (Tokyo, Japan). Neuraminidase was purchased from Nakalai Tesque (Kyoto, Japan). *N*-glycosidase F (PNGaseF) and endoproteinase Asp-N (Asp-N) were purchased from Boehringer Mannheim (Mannheim, Germany). All other chemicals were obtained from commercial sources and were of the highest purity available.

2.2. Establishment of a CHO cell line expressing rhFS

Complementary DNA encoding human FS288, was constructed from FS315 cDNA, and was cloned into pcDNA3.1/Hygro. This expression vector was transfected into CHO cells with LipofectAMINE plus reagent, according to the manufacturer's instructions. To screen the transformants, the transfectants were cultured with Ham's F12 medium supplemented with 10% FCS and 1 mg/ml hygromycin. After 2 weeks, the colonies were lifted with a micropipette. Expression levels of rhFS were assessed by an activin-neutralizing assay. The candidates were cloned by limiting dilution twice and were assessed again. The most productive rhFS-expressing clone (CHO-FS) was used in the following experiments.

2.3. Preparation of rhFS

Semi-confluent CHO-FS cells were cultured in Ham's F12 medium supplemented with 2% FCS. The conditioned medium was concentrated to a 1/10 volume by filtration with a Pellicon XL membrane (M_r 5000 cut), and was applied onto a sulfated-cellulofine column (2.5 × 20 cm) at 2 ml/min. The column was washed with 50 mM Tris–HCl (pH 8) containing 0.5 M NaCl, and the protein was eluted with 50 mM Tris–HCl (pH 8) containing 1.5 M NaCl. The effluent from the column was fractionated, and rhFS was monitored on Western blots using polyclonal anti-FS antibody. The fractions containing rhFS were injected into an HPLC (Hitachi D7000, Hitachi Co., Tokyo, Japan) apparatus equipped with a reversed-phase column (Vydac C4, 10 × 300 mm, The Separations Group, Inc., Hesperia, CA, USA). The protein was eluted with a linear gradient of 16–48% of acetonitrile/0.1% trifluoroacetic acid (TFA) for 30 min at a flow rate of 2 ml/min. Elution of proteins was monitored at 280 nm and individual peaks were manually collected. Fraction of rhFS was monitored on Western blots using polyclonal anti-FS antibody.

2.4. SDS-PAGE analysis of rhFS

RhFS was digested with or without PNGaseF at 37 °C for 24 h. The proteins were separated by sodium dodecyl sulfate-polyacrylamide gel electrophoresis

(SDS-PAGE) on 10% polyacrylamide gel. The gel was stained with Coomassie blue.

2.5. Isoelectric focusing

RhFS was dissolved in 100 mM ammonium acetate buffer, pH 4.5, and incubated with neuraminidase at 37 °C for 18 h. The proteins were precipitated with cold acetone and separated by isoelectric focusing (IEF). The gel was stained with Coomassie blue.

2.6. MALDI-TOF MS

RhFS (20 µg) was subjected to positive-ion matrix-assisted laser desorption/ionization time-of-flight mass spectrometry (MALDI-TOF MS), using a Shimazu/KRATOS MALDI I instrument (Shimazu Co., Kyoto, Japan) with 3,5-dimethoxy-4-hydroxy-cinnamic acid as the matrix.

2.7. Monosaccharide composition analysis

Monosaccharide composition analysis was performed according to the method reported by Hardy et al. [23]. Briefly, rhFS (50 µg) was hydrolyzed with 2 M TFA at 100 °C for 3 h. Monosaccharide compositions were analyzed by high-pH anion-exchange chromatography with pulsed amperometric detection (HPAEC-PAD) using a DX-300 system (Dionex, Sunnyvale, CA, USA) equipped with a CarboPac PA-1 anion exchange column (4 × 250 mm, Dionex).

2.8. Preparation of N-linked oligosaccharides alditols

N-linked oligosaccharides alditols were prepared by a previously described method [20]. Briefly, rhFS (100 µg) was digested with 5 units of PNGaseF at 37 °C for 2 days. Proteins were precipitated with 75% cold ethanol. The oligosaccharides were incubated with $NaBH_4$ at room temperature for 2 h. Excess reagent was decomposed with diluted acetic acid. The mixture was applied to a Supelclean ENVI-Carb column (Supelco, Bellefonte, PA, USA), which was washed with H_2O to remove the salts. Borohydride-reduced oligosaccharides were eluted with 30% acetonitrile/5 mM ammonium acetate.

2.9. Sugar profiling by LC/MS

Sugar profiling was carried out using a MAGIC 2002 system (Michrom BioResources, Inc., Auburn, CA, USA) connected to a TSQ7000 triple-stage quadruple mass spectrometer (ThermoFinnigan, San Jose, CA, USA) in the positive-ion mode. The column used was a GCC (Hypercarb 5 µm, 1.0 × 150 mm, ThermoFinnigan). The eluents were 5 mM ammonium acetate (pH 9.6) containing 2% acetonitrile (pump A); and 5 mM ammonium acetate (pH 9.6) containing 80% acetonitrile (pump B). The N-linked oligosaccharide alditols were eluted at a flow rate of 50 µl/min for 80 min with a gradient of 5–30% in pump B. The ESI voltage was set at 4500 V, and the capillary temperature was 175 °C. The electron multiplier was set at 1200 V.

2.10. Asp-N digestion

RhFS was reduced and S-carboxymethylated as previously described [20]. Briefly, rhFS (100 µg) was dissolved in 0.5 M Tris–HCl buffer (pH 8.6) containing 8 M guanidine and 5 mM EDTA. After reduction with 2-mercaptoethanol at room temperature for 2 h, monoiodoacetic acid was added and incubated at room temperature for 2 h in the dark. Reduced and S-carboxymethylated-rhFS (equivalent to 100 µg of rhFS) was digested with Asp-N (2 µg) in 25 mM NH_4HCO_3 (pH 8.0) at 37 °C for 20 h. The predicted peptides to be obtained by Asp-N digestion were sequentially designated as D1–D15 (Fig. 1).

2.11. Peptide/glycopeptide mapping of Asp-N-digested rhFS

Peptide/glycopeptide mapping was carried out using a MAGIC 2002 system connected to a TSQ7000 triple-stage quadruple mass spectrometer in the positive-ion mode. The column used was a MAGIC C18 column (1.0 × 150 mm, Michrom BioResources). The eluents were 2% acetonitrile/0.05% TFA (pump A), and 80% acetonitrile/0.05% TFA (pump B). Asp-N-digested rhFS was eluted with a linear gradient from 5 to 45% in pump B at a flow rate of 50 µl/min for 40 min. The eluate was monitored at 206 nm. The ESI voltage was set at 4500 V, and the capillary temperature was 175 °C. The electron multiplier was set at 1200 V. Precursor-ion scanning was performed using argon gas as the collision gas at a pressure of 2 mTorr. The collision energy was adjusted to −25 eV. The scan rate was 3 s/scan.

3. Results

3.1. Heterogeneity of rhFS

The carbohydrate heterogeneity of rhFS was analyzed by SDS-PAGE with and without PNGaseF digestion. The intact rhFS migrated as bands of an apparent molecular mass of 32 kDa and 33–36 kDa under non-reducing conditions (Fig. 2A, lane 1). PNGaseF digestion resulted in the disappearance of the multiple bands at 33–36 kDa with increases in the 32-kDa band (Fig. 2A, lane 2). These results suggest that the 32 kDa band and higher molecular weight bands are

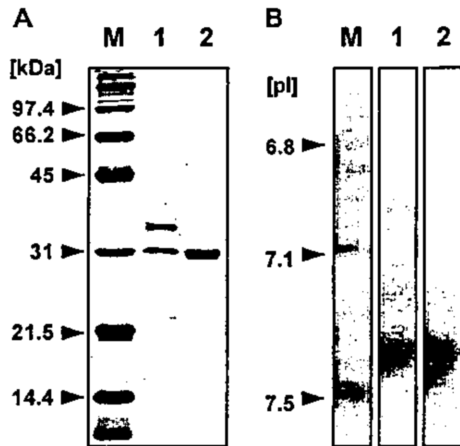

Fig. 2. (A) SDS-PAGE analysis of intact rhFS (lane 1) and PNGaseF-digested rhFS (lane 2). Lane M represents molecular weight markers. (B) IEF of intact rhFS (lane 1) and neuraminidase-digested rhFS (lane 2). Lane M represents p*I* markers.

the non-glycosylated FS and the glycosylated FS with diverse N-linked oligosaccharides, respectively.

The sialic acid heterogeneity of rhFS was analyzed by IEF with and without neuraminidase digestion. IEF of intact rhFS showed that the majority of the isoforms are located from p*I* 6.9 to 7.4 (Fig. 2B, lane 1). After treatment with neuraminidase, the acidic bands had disappeared and shifted at p*I* 7.4 (Fig. 2B, lane 2). These results suggested that the sialic acids contribute to the heterogeneity and the charge of rhFS.

The distribution of glycoforms was further investigated by MALDI-TOF MS. As shown in Fig. 3, multiple ions were detected in the range of 31.5–37 kDa. The most abundant ion at *m/z* 31,525 corresponded to the theoretical mass of non-glycosylated FS (31,514 Da). The other ions at *m/z* 33,804 and 35,600 could have

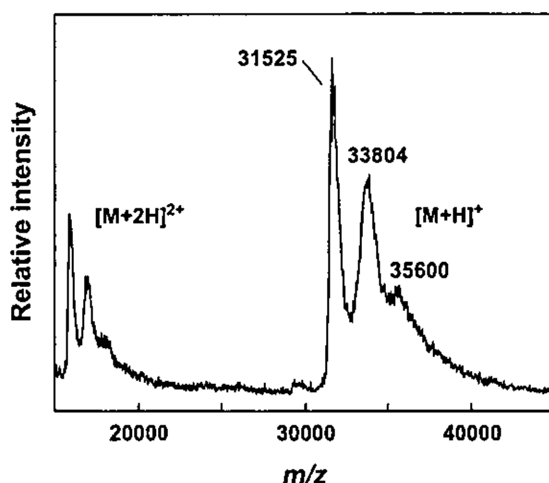

Fig. 3. MALDI-TOF MS analysis of intact rhFS. The peaks at *m/z* 31,525, 33,804 and 35,600 correspond to the non-glycosylated and glycosylated form of rhFS, respectively.

been monoglycosylated FS and diglycosylated FS, respectively.

3.2. Monosaccharide composition of rhFS

Monosaccharide composition was analyzed by hydrolysis followed by HPAEC-PAD. The relative molecular ratio of fucose and glucosamine were estimated at 1.2 and 4.4, respectively, when mannose was considered as 3.0 (Table 1). This result suggests the presence of fucosylated bi- and triantennary-type oligosaccharides. No galactosamine residue was detected, suggesting the absence of O-linked oligosaccharides.

3.3. N-linked oligosaccharides in rhFS

N-linked oligosaccharides were released from rhFS by PNGaseF digestion and reduced with $NaBH_4$ to avoid the separation of anomers. Then the oligosaccharide alditols from rhFS were analyzed by GCC-LC/MS. Fig. 4 shows the total ion current chromatogram of N-linked oligosaccharide alditols. The *m/z* values of intense ions observed in major peaks (peaks 8 and 12) were 1040.7^{2+} and 1186.4^{2+}, which were consistent with the theoretical *m/z* values of $[dHex][Hex]_5[HexNAc]_4[NeuAc]^{2+}$ and $[dHex][Hex]_5[HexNAc]_4[NeuAc]_2{}^{2+}$, respectively (Table 2). The elution times of these oligosaccharides were in good agreement with those of fucosyl biantennary oligosaccharides bearing mono- and di-NeuAc prepared from erythropoietin, respectively [24]. An ion at *m/z* 1041.4^{2+} was also detected in peak 6. This oligosaccharide could be a sialylation isomer of peak 8 (1040.7^{2+}).

Likewise, the ions at *m/z* 1790.7^{+} and 895.4^{2+} in peak 2 and at *m/z* 1077.9^{2+} in peak 3 were assigned as an asialo fucosylated biantennary oligosaccharide and an asialo fucosylated triantennary oligosaccharide, respectively. The ion at *m/z* 2389.6^{+} and 1194.6^{2+} in peak 11 was consistent with $[dHex][Hex]_5[HexNAc]_4[NeuAc][NeuGc]^{2+}$ or $[Hex]_6[HexNAc]_4[NeuAc]_2{}^{2+}$, respectively. The ions at *m/z* 2097.7^{+} and 1048.6^{2+} in peak 5 and at *m/z* 2096.5^{+} and 1049.5^{2+} in peak 8 were consistent with $[dHex][Hex]_5[HexNAc]_4[NeuGc]^{2+}$ or $[Hex]_6[HexNAc]_4[NeuAc]^{2+}$, respectively. The minor ions at *m/z* 1224.1^{2+}, 1224.3^{2+}, 1369.7^{2+}, 1369.8^{2+},

Table 1
Monosaccharide composition analysis of rhFS oligosaccharides

Monosaccharide	Relative molar proportions[a]
Fucose	1.2
Galactosamine	0.3
Glucosamine	4.4
Galactose	3.2
Glucose	0.3
Mannose	3.0

[a] Data are normalized to three-mannose residues.

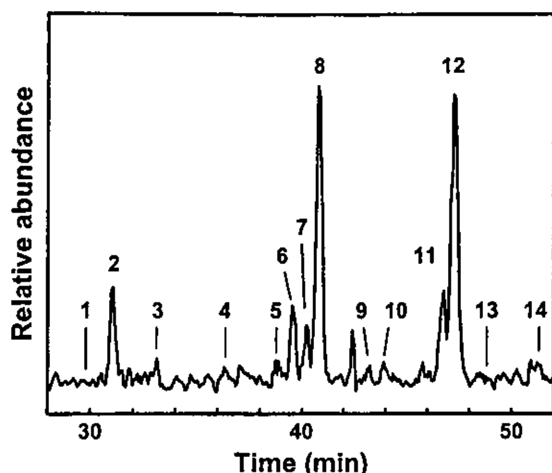

Fig. 4. Sugar map of oligosaccharide alditols released from rhFS. N-linked oligosaccharide alditols from rhFS were separated with GCC. The total ion content was scanned using the positive-ion mode at m/z 700–2400.

Table 2
Putative structures of N-linked oligosaccharides deduced from the GCC-LC/MS

Peak No.[a]	Carbohydrate structure[b]	Theoretical mass[c]	Observed mass[d]		
			M^+	M^{2+}	M^{3+}
1		1627.5	1628.3	814.2	-
2		1789.7	1790.7	895.4	-
3		2155.0	-	1077.9	-
4		1934.7	-	967.9	-
5	*1	2096.9	2097.7	1048.6	-
6		2080.9	2081.2	1041.4	-
7		2446.3	-	1224.1	817.4
8	*1	2096.9	2096.5	1049.6	-
		2080.9	2082.2	1040.7	-
9		2446.3	-	1224.3	-
10		2226.0	-	1114.2	-
11	*2	2388.2	2389.6	1194.6	-
		2737.5	-	1369.7	913.4
12		2372.2	2372.2	1186.4	-
		2737.5	-	1369.8	-
13		2737.5	-	1370.5	913.8
14		3028.8	-	1515.5	-

Note: The observed m/z of *1 and *2 are also consistent with the theoretical m/z value of $[Hex]_6[HexNAc]_4[NeuAc]$ and $[Hex]_6[HexNAc]_4[NeuAc]_2$, respectively.

[a] Peak label in Fig. 4.

[b] Proposed structures based on molecular weight. Symbols: solid squares, GlcNAc; open circles, mannose; open diamonds, galactose; dotted diamonds, fucose; solid circle, NeuAc; dotted circle, NeuGc.

[c] Calculated average mass.

[d] Mass of the ion measured in the positive-ion ESI mass spectrum from alditols.

1370.5^{2+} and 1515.5^{2+} in peaks 7, 9, 11, 12, 13 and 14 were deduced to the fucosylated triantennary oligosaccharides with NeuAc, respectively.

The ratio of oligosaccharides was estimated as follows: fucosylated biantennary, ca. 85%, and fucosylated triantennary structures, ca. 10%, based on their ion currents; these results were in good agreement with the results of the monosaccharide composition analysis.

3.4. Site-specific glycosylation of rhFS

FS contains two potential *N*-glycosylation sites (Asn95 and Asn259, Fig. 1). The site-specific glycosylation and other post-translational modifications, such as phosphorylation and hydroxylation, were analyzed by mass spectrometric peptide/glycopeptide mapping (Fig. 5a, Table 3). Most of the non-glycosylated peptides were detected except for the small peptides, i.e. peptides D2 (tripeptide), D13 (tetrapeptide), and D12 (pentapeptide), which suggests the absence of *O*-glycans and any post-translational modifications on these peptides. The small peptides have no putative *N*-glycosylation site (Fig. 1), and no galactosamine residue was detected (Table 1). These findings suggest the absence of N- and O-linked oligosaccharides. However, the possibility remains that the small peptides are modified, such as by phosphorylation. Two unpredicted peptides (m/z 1176.2^{2+} and 510.4^{2+}) were detected among the Asp-N digests of rhFS. They were assigned to peptides D15-1 and D15-2, which were produced from peptide D15 by further cleavage at the amino-terminal of Glu280. It was reported that a cleavage at the N-terminal site of glutamic acid is a possible cut site for Asp-N under the same conditions [25]. Peptides D5 and D15-1, each of which have potential glycosylation site, were detected as non-glycosylated forms in the peptide/glycopeptide map.

Precursor-ion scanning, which can detect $[Hex][HexNAc]^+$ at m/z 366 produced by collision-induced dissociation, was performed for the monitoring of the glycopeptides. The TIC chromatogram of the precursor-ion scanning showed two significant peaks, peaks G1 and G2 (Fig. 5b). Fig. 6 shows the mass spectra of peaks G1 and G2 in Fig. 5b. On the basis of the theoretical masses of the peptides and oligosaccharides identified by sugar mapping (Table 2), peaks G1 and G2

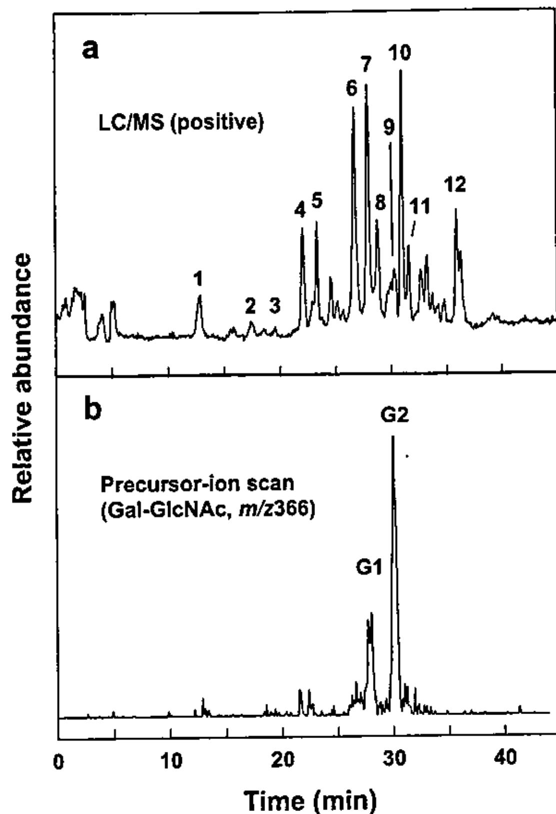

Fig. 5. Peptide/glycopeptide map of the rhFS Asp-N digest. The total ion current chromatogram of LC/MS in the positive-ion mode at m/z 400–2400 (a), and the TIC chromatogram of LC/MS/MS, precursor-ion scan of m/z 366 (b).

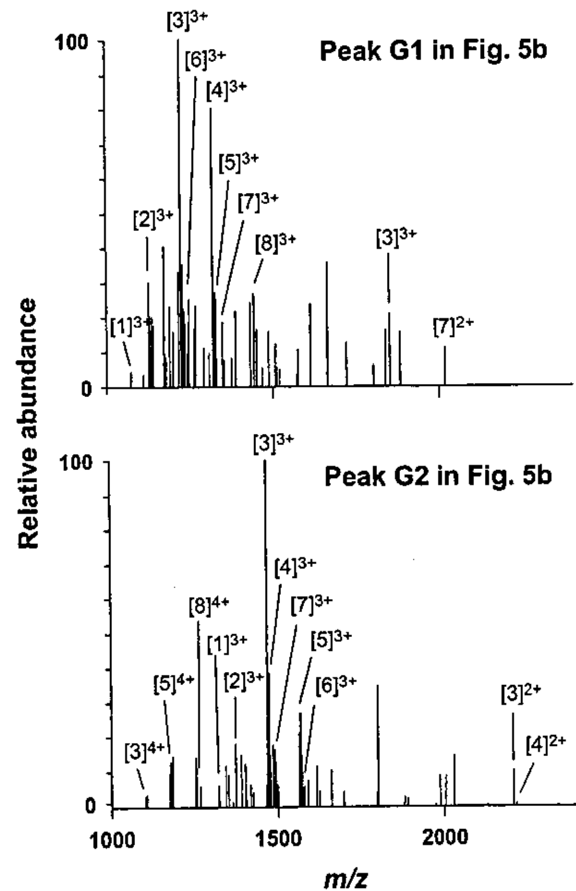

Fig. 6. Mass spectra of glycopeptides in peaks G1 and G2 in Fig. 5b. The observed m/z value of each ion is summarized in Table 4.

were assigned to glycosylated D5 and D15-1, respectively. The oligosaccharides attached to each N-glycosylation site were deduced as shown in Table 4. By comparing the N-linked oligosaccharide structures on Asn95 with those on Asn259, it was concluded that biantennary oligosaccharides are major oligosaccharides located at both Asn95 and Asn259, whereas the triantennary structures are present mainly at Asn95.

Table 3
Assignment of the peaks in Fig. 5a

Peak no.[a]	Peptide[b]	Theoretical mass[c]	Observed m/z[d]					
			M^{+}	M^{2+}	M^{3+}	M^{4+}	M^{5+}	M^{6+}
1	D4	2666.0	–	1334.2	889.9	667.4	–	–
2	D14	777.8	778.6	–	–	–	–	–
3	D15-2[e]	1018.0	1019.0	510.4	–	–	–	–
4	D11	1456.6	1457.5	729.0	486.3	–	–	–
5	D6	4378.8	–	–	1460.8	1095.5	–	–
6	D8	3326.4	–	1664.6	1109.5	–	–	–
	D10	1467.6	1468.2	734.8	490.1	–	–	–
7	D1	4728.1	–	–	1577.0	1183.2	947.0	789.6
8	D7	1329.4	1330.2	665.3	–	–	–	–
9	D5	1608.7	1609.3	805.1	–	–	–	–
10	D9	4165.6	–	–	1389.0	1042.2	834.1	–
11	D15-1[e]	2350.6	–	1176.2	784.2	–	–	–
12	D3	3219.5	–	1610.1	1073.8	806.4	–	–

[a] Peak label in Fig. 5a.
[b] Predicted peptides were shown in Fig. 1.
[c] Calculated average mass.
[d] Mass of the ions measured in the positive-ion ESI mass spectrum from precursor-ion scan.
[e] Peptide derived from D15 peptide.

4. Discussion

The aim of the present study was to analyze the distribution of the glycoforms and the carbohydrate structures of rhFS. Previous study of FS isolated from porcine ovary has shown that porcine FS exists in six isoforms, due to alternative splicing and the site occupancy of N-linked oligosaccharides [8]. In this study, we used rhFS288 to eliminate the heterogeneity due to alternative splicing. The results of SDS-PAGE and MALDI-TOF MS revealed the presence of both non-glycosylated and glycosylated forms (Figs. 2 and 3). FS contains two potential *N*-glycosylation sites. Using mass spectrometric peptide/glycopeptide mapping and precursor-ion scanning, we found that both *N*-glycosylation sites were partially glycosylated (Fig. 5 and Table 3). Non-glycosylated and glycosylated proteins containing Asn95 and Asn259 were detected in the peptide/glycopeptide map and precursor-ion scanning, respectively. Monosaccharide composition analyses suggested the presence of linkages of fucosylated bi- and triantennary complex-type oligosaccharides on rhFS (Table 1). This finding was supported by mass spectrometric oligosaccharide profiling, in which the m/z values and elution times of some of the oligosaccharides from rhFS were in good agreement with those of standard oligosaccharides. The site-specific glycosylations were deduced on the basis of the mass spectra of glycopeptides. It was suggested that biantennary oligosaccharides attach to both Asn95 and Asn259, whereas triantennary oligosaccharides attach mainly to Asn95 (Fig. 6 and Table 4).

Asn95 is located in the follistatin domain I, which is thought to be the heparin-binding site [26]. The site occupancy and structure of N-linked oligosaccharides on Asn95 may affect the heparin-binding ability of FS. Heparin/heparan sulfate proteoglycans are known to exert an important influence on FS, which neutralizes the activity of activins. It is therefore possible that sialylated oligosaccharides at Asn95 control the activin-neutralizing activity via modulation of the heparin-binding ability of FS. In fact, it was reported that the *N*-glycosylation isoforms of antithrombin and heparin cofactor II differ substantially in their affinity for heparin [27,28]. We are currently studying the role played by oligosaccharides in the activin-neutralizing activity of FS; these studies employ the carbohydrate remodeling technique using the CHO cell line established in the present study.

Table 4
Putative structures of N-linked oligosaccharides deduced from the LC/MS of the glycopeptides corresponding to the Asn95 and Asn259

Carbohydrate Structure[a]	Asn95					Asn259				
	Ions in peak G1	Theoretical mass[b]	Observed m/z [c]			Ions in peak G2	Theoretical mass[b]	Observed m/z		
			M^{2+}	M^{3+}	M^{4+}			M^{2+}	M^{3+}	M^{4+}
	1	3216.2	-	1073.4	-	1	3958.1	-	1319.6	-
	2	3378.6	-	1126.6	-	2	4120.5	-	1373.9	-
	3	3669.6	1835.7	1223.2	-	3	4411.5	2206.3	1471.8	1104.7
	-		-		-	4	4427.5	2214.8	1475.7	-
	4	3960.9	-	1320.6	-	5	4702.8	-	1569.5	1177.1
	5	3976.6	-	1326.8	-	6	4718.8	-	1574.5	-
	6	3743.7	-	1248.6	-	7	4485.6	-	1497.2	-
	7	4034.9	2017.5	1346.9	-	-	-	-	-	-
	8	4326.2	-	1444.1	-	8	5068.1	-	-	1267.6

[a] Proposed structures based on molecular weight. Symbols: solid squares, GlcNAc; open circles, mannose; open diamonds, galactose; dotted diamonds, fucose; solid circle, NeuAc; dotted circle, NeuGc.
[b] Calculated average mass.
[c] Mass of the ion measured in the positive-ion ESI mass spectrum from precursor-ion scan. Mass spectra were shown in Fig. 6.

Acknowledgements

We thank Dr. Y. Eto (Ajinomoto Co., Inc.) for providing the human FS315 cDNA. This work was supported by a grant-in-aid for the Research on Health Sciences Focusing on Drug Innovation from the Japan Health Sciences Foundation.

References

[1] Robertson DM, Klein R, de Vos FL, McLachlan RI, Wettenhall RE, Hearn MT, et al. The isolation of polypeptides with FSH suppressing activity from bovine follicular fluid which are structurally different to inhibin. Biochem Biophys Res Commun 1987;149:744–9.
[2] Ueno N, Ling N, Ying SY, Esch F, Shimasaki S, Guillemin R. Isolation and partial characterization of follistatin: a single-chain Mr 35,000 monomeric protein that inhibits the release of follicle-stimulating hormone. Proc Natl Acad Sci USA 1987;84: 8282–6.
[3] Nakamura T, Takio K, Eto Y, Shibai H, Titani K, Sugino H. Activin-binding protein from rat ovary is follistatin. Science 1990; 247:836–8.
[4] Kogawa K, Nakamura T, Sugino K, Takio K, Titani K, Sugino H. Activin-binding protein is present in pituitary. Endocrinology 1991;128:1434–40.
[5] Massague J. The transforming growth factor-beta family. Annu Rev Cell Biol 1990;6:597–641.
[6] Kingsley DM. The TGF-beta superfamily: new members, new receptors, and new genetic tests of function in different organisms. Genes Dev 1994;8:133–46.
[7] Wada M, Shintani Y, Kosaka M, Sano T, Hizawa K, Saito S. Immunohistochemical localization of activin A and follistatin in human tissues. Endocr J 1996;43:375–85.
[8] Sugino K, Kurosawa N, Nakamura T, Takio K, Shimasaki S, Ling N, et al. Molecular heterogeneity of follistatin, an activin-binding protein. Higher affinity of the carboxyl-terminal truncated forms for heparan sulfate proteoglycans on the ovarian granulosa cell. J Biol Chem 1993;268:15579–87.
[9] Patel K. Follistatin. Int J Biochem Cell Biol 1998;30:1087–93.
[10] Inouye S, Guo Y, DePaolo L, Shimonaka M, Ling N, Shimasaki S. Recombinant expression of human follistatin with 315 and 288 amino acids: chemical and biological comparison with native porcine follistatin. Endocrinology 1991;129:815–22.
[11] Sumitomo S, Inouye S, Liu XJ, Ling N, Shimasaki S. The heparin binding site of follistatin is involved in its interaction with activin. Biochem Biophys Res Commun 1995;208:1–9.
[12] Hashimoto O, Nakamura T, Shoji H, Shimasaki S, Hayashi Y, Sugino H. A novel role of follistatin, an activin-binding protein, in the inhibition of activin action in rat pituitary cells. Endocytotic degradation of activin and its acceleration by follistatin associated with cell-surface heparan sulfate. J Biol Chem 1997;272: 13835–42.
[13] Kobata A. Structures and functions of the sugar chains of glycoproteins. Eur J Biochem 1992;209:483–501.
[14] Varki A. Biological roles of oligosaccharides: all of the theories are correct. Glycobiology 1993;3:97–130.
[15] Itoh S, Kawasaki N, Ohta M, Hyuga M, Hyuga S, Hayakawa T. Study on evaluating methods for the quality control of glycoprotein products. (III)—Erythropoietin products. Part 3. Bull Natl Inst Health Sci 2001;65–9.
[16] Simultaneous microanalysis of N-linked oligosaccharides in a glycoprotein using microbore graphitized carbon column liquid chromatography–mass spectrometry. J Chromatogr A 2002;968: 89–100.
[17] Kawasaki N, Ohta M, Hyuga S, Hashimoto O, Hayakawa T. Analysis of carbohydrate heterogeneity in a glycoprotein using liquid chromatography/mass spectrometry and liquid chromatography with tandem mass spectrometry. Anal Biochem 1999;269: 297–303.
[18] Kawasaki N, Ohta M, Hyuga S, Hyuga M, Hayakawa T. Application of liquid chromatography/mass spectrometry and liquid chromatography with tandem mass spectrometry to the analysis of the site-specific carbohydrate heterogeneity in erythropoietin. Anal Biochem 2000;285:82–91.
[19] Kawasaki N, Haishima Y, Ohta M, Itoh S, Hyuga M, Hyuga S, et al. Structural analysis of sulfated N-linked oligosaccharides in erythropoietin. Glycobiology 2001;11:1043–9.
[20] Kawasaki N, Ohta M, Itoh S, Hyuga M, Hyuga S, Hayakawa T. Usefulness of sugar mapping by liquid chromatography/mass spectrometry in comparability assessments of glycoprotein products. Biologicals 2002;30:113–23.
[21] Ohta M, Kawasaki N, Hyuga S, Hyuga M, Hayakawa T. Selective glycopeptide mapping of erythropoietin by on-line high-performance liquid chromatography–electrospray ionization mass spectrometry. J Chromatogr A 2001;910:1–11.
[22] Ohta M, Kawasaki N, Itoh S, Hayakawa T. Usefulness of glycopeptide mapping by liquid chromatography/mass spectrometry in comparability assessment of glycoprotein products. Biologicals 2002;30:235–44.
[23] Hardy MR, Townsend RR, Lee YC. Monosaccharide analysis of glycoconjugates by anion exchange chromatography with pulsed amperometric detection. Anal Biochem 1988;170:54–62.
[24] Kawasaki N, Ohta M, Hyuga S, Hyuga M, Hayakawa T. Application of liquid chromatography/mass spectrometry and liquid chromatography with tandem mass spectrometry to the analysis of the site-specific carbohydrate heterogeneity in erythropoietin. Anal Biochem 2000;285:82–91.
[25] Ingrosso D, Fowler AV, Bleibaum J, Clarke S. Specificity of endoproteinase Asp-N (Pseudomonas fragi): cleavage at glutamyl residues in two proteins. Biochem Biophys Res Commun 1989; 162:1528–34.
[26] Inouye S, Ling N, Shimasaki S. Localization of the heparin binding site of follistatin. Mol Cell Endocrinol 1992;90:1–6.
[27] Picard V, Ersdal-Badju E, Bock SC. Partial glycosylation of antithrombin III asparagine-135 is caused by the serine in the third position of its *N*-glycosylation consensus sequence and is responsible for production of the beta-antithrombin III isoform with enhanced heparin affinity. Biochemistry 1995;34:8433–40.
[28] Bohme C, Nimtz M, Grabenhorst E, Conradt HS, Strathmann A, Ragg H. Tyrosine sulfation and *N*-glycosylation of human heparin cofactor II from plasma and recombinant Chinese hamster ovary cells and their effects on heparin binding. Eur J Biochem 2002;269:977–88.

Available online at www.sciencedirect.com

SCIENCE @ DIRECT®

Biologicals 32 (2004) 70–77

BIOLOGICALS

www.elsevier.com/locate/biologicals

Analysis of site-specific glycosylation in recombinant human follistatin expressed in Chinese hamster ovary cells

Masashi Hyuga*, Satsuki Itoh, Nana Kawasaki, Miyako Ohta, Akiko Ishii, Sumiko Hyuga, Takao Hayakawa

Division of Biological Chemistry and Biologicals, National Institute of Health Sciences, 1-18-1, Kamiyoga, Setagaya-ku, Tokyo 158-8501, Japan

Received 22 October 2003; accepted 1 April 2004

Abstract

Follistatin (FS), a glycoprotein, plays an important role in cell growth and differentiation through the neutralization of the biological activities of activins. In this study, we analyzed the glycosylation of recombinant human FS (rhFS) produced in Chinese hamster ovary cells. The results of SDS-PAGE and MALDI-TOF MS revealed the presence of both non-glycosylated and glycosylated forms. FS contains two potential *N*-glycosylation sites, Asn95 and Asn259. Using mass spectrometric peptide/glycopeptide mapping and precursor-ion scanning, we found that both *N*-glycosylation sites were partially glycosylated. Monosaccharide composition analyses suggested the linkages of fucosylated bi- and triantennary complex-type oligosaccharides on rhFS. This finding was supported by mass spectrometric oligosaccharide profiling, in which the *m/z* values and elution times of some of the oligosaccharides from rhFS were in good agreement with those of standard oligosaccharides. Site-specific glycosylation was deduced on the basis of the mass spectra of the glycopeptides. It was suggested that biantennary oligosaccharides are major oligosaccharides located at both Asn95 and Asn259, whereas the triantennary structures are present mainly at Asn95.
© 2004 The International Association for Biologicals. Published by Elsevier Ltd. All rights reserved.

Abbreviations: CHO, Chinese hamster ovary; FCS, fetal calf serum; FS, follistatin; GCC, graphitized carbon column; GnT, *N*-acetylglucosaminyltransferase; HPAEC-PAD, high-pH anion-exchange chromatography with pulsed amperometric detection; IEF, isoelectric focusing; LC/MS, liquid chromatography/mass spectrometry; MALDI-TOF MS, matrix-assisted laser desorption/ionization time-of-flight mass spectrometry; NeuAc, *N*-acetyl neuraminic acid; NeuGc, *N*-glucoryl neuraminic acid; PNGaseF, peptide *N*-glycanase F; rhFS, recombinant human follistatin; SDS-PAGE, sodium dodecyl sulfate-polyacrylamide gel electrophoresis; TFA, trifluoroacetic acid

1. Introduction

Follistatin (FS), a glycoprotein, was first discovered in ovarian follicular fluid as an inhibitor of pituitary follicle-stimulating hormone secretion [1,2]. Subsequent studies have revealed that FS can bind to activins and neutralize their biological activities [3,4]. Activins are members of the transforming growth factor-β superfamily, and they play important roles in the regulation of cell growth and in the differentiation processes that lead to morphogenesis in early vertebrate development [5,6]. Since FS and activins are broadly distributed, they are not confined solely to tissues associated with reproduction [7].

FS is present in heterogeneous forms [8]. The FS gene consists of 315 amino acids, and it includes six exons (Fig. 1); alternative splicing can generate two isoforms, i.e. a 315-amino-acid protein (the full-length form, FS315) and a 288-amino-acid protein (the carboxy-truncated form, FS288) [9]. The activin-neutralizing activity of FS288 is higher than that of FS315 [10,11], which appears to correlate with their heparin/heparan sulfate proteoglycan-binding abilities [12]. The heterogeneity of FS is also due to diverse glycosylation. FS has two potential *N*-glycosylation sites (Asn95 and Asn259). Oligosaccharides are generally known to play important roles in defining the properties of glycoproteins such as their biological activity, immunogenicity,

* Corresponding author. Fax: +81-3-3700-9084.
E-mail address: mhyuga@nihs.go.jp (M. Hyuga).

1045-1056/04/$30.00 © 2004 The International Association for Biologicals. Published by Elsevier Ltd. All rights reserved.
doi:10.1016/j.biologicals.2004.04.001

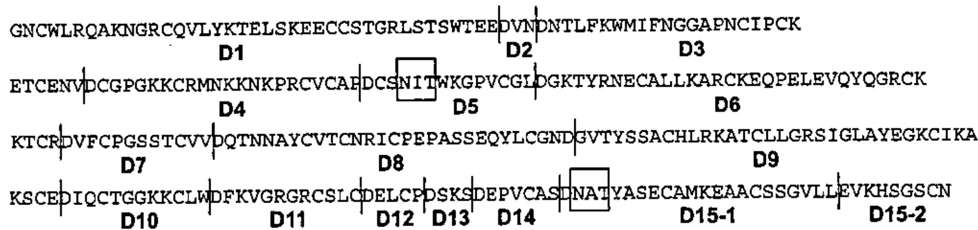

Fig. 1. Amino acid sequence of rhFS. Predicted cleavage sites with Asp-N are indicated by |. The potential N-glycosylation sites are indicated by boxes.

pharmacokinetics, solubility, and protease resistance [13,14]. Glycosylation on FS is also likely to exert an effect on activin-neutralizing activity; however, neither structure of the N-linked oligosaccharides in FS, nor their physiological roles, have been clarified due to the limited availability of these oligosaccharides.

The aim of this study was to elucidate the glycosylation of FS. We previously developed an oligosaccharide profiling method using liquid chromatography/mass spectrometry (LC/MS) equipped with a graphitized carbon column (GCC) [15–22]. Recently, we demonstrated a procedure for facilitating the structural analysis of glycoproteins [16]. Carbohydrate profiles and site-specific glycosylations can be characterized by the GCC-LC/MS method, followed by mass spectrometric peptide/glycopeptide mapping. We used this method to demonstrate here the carbohydrate heterogeneity and the site-specific N-linked oligosaccharide structures in recombinant human FS288 (rhFS) produced in Chinese hamster ovary (CHO) cells, in which a sufficient amount of FS could be expressed.

2. Materials and methods

2.1. Materials

Human FS315 cDNA and recombinant human activin A were kindly provided by Dr. Yuzuru Eto (Ajinomoto Co., Inc., Kawasaki, Japan). CHO cells were obtained from the Japanese Cancer Research Resources Bank (Tokyo, Japan). Mammalian expression vector pcDNA3.1/Hygro was purchased from Invitrogen (Carlsbad, CA, USA). LipofectAMINE plus reagent, Ham's F12 medium, fetal calf serum (FCS) and hygromycin were purchased from Life Technologies Inc. (Rockville, MD, USA). Pellicon XL membrane and Immobilon-P membrane were purchased from Millipore Corp. (Bedford, MA, USA). Sulfated-cellulofine was purchased from Seikagaku Corp. (Tokyo, Japan). Neuraminidase was purchased from Nakalai Tesque (Kyoto, Japan). *N*-glycosidase F (PNGaseF) and endoproteinase Asp-N (Asp-N) were purchased from Boehringer Mannheim (Mannheim, Germany). All other chemicals were obtained from commercial sources and were of the highest purity available.

2.2. Establishment of a CHO cell line expressing rhFS

Complementary DNA encoding human FS288, was constructed from FS315 cDNA, and was cloned into pcDNA3.1/Hygro. This expression vector was transfected into CHO cells with LipofectAMINE plus reagent, according to the manufacturer's instructions. To screen the transformants, the transfectants were cultured with Ham's F12 medium supplemented with 10% FCS and 1 mg/ml hygromycin. After 2 weeks, the colonies were lifted with a micropipette. Expression levels of rhFS were assessed by an activin-neutralizing assay. The candidates were cloned by limiting dilution twice and were assessed again. The most productive rhFS-expressing clone (CHO-FS) was used in the following experiments.

2.3. Preparation of rhFS

Semi-confluent CHO-FS cells were cultured in Ham's F12 medium supplemented with 2% FCS. The conditioned medium was concentrated to a 1/10 volume by filtration with a Pellicon XL membrane (M_r 5000 cut), and was applied onto a sulfated-cellulofine column (2.5 × 20 cm) at 2 ml/min. The column was washed with 50 mM Tris–HCl (pH 8) containing 0.5 M NaCl, and the protein was eluted with 50 mM Tris–HCl (pH 8) containing 1.5 M NaCl. The effluent from the column was fractionated, and rhFS was monitored on Western blots using polyclonal anti-FS antibody. The fractions containing rhFS were injected into an HPLC (Hitachi D7000, Hitachi Co., Tokyo, Japan) apparatus equipped with a reversed-phase column (Vydac C4, 10 × 300 mm, The Separations Group, Inc., Hesperia, CA, USA). The protein was eluted with a linear gradient of 16–48% of acetonitrile/0.1% trifluoroacetic acid (TFA) for 30 min at a flow rate of 2 ml/min. Elution of proteins was monitored at 280 nm and individual peaks were manually collected. Fraction of rhFS was monitored on Western blots using polyclonal anti-FS antibody.

2.4. SDS-PAGE analysis of rhFS

RhFS was digested with or without PNGaseF at 37 °C for 24 h. The proteins were separated by sodium dodecyl sulfate-polyacrylamide gel electrophoresis

(SDS-PAGE) on 10% polyacrylamide gel. The gel was stained with Coomassie blue.

2.5. *Isoelectric focusing*

RhFS was dissolved in 100 mM ammonium acetate buffer, pH 4.5, and incubated with neuraminidase at 37 °C for 18 h. The proteins were precipitated with cold acetone and separated by isoelectric focusing (IEF). The gel was stained with Coomassie blue.

2.6. *MALDI-TOF MS*

RhFS (20 µg) was subjected to positive-ion matrix-assisted laser desorption/ionization time-of-flight mass spectrometry (MALDI-TOF MS), using a Shimazu/KRATOS MALDI I instrument (Shimazu Co., Kyoto, Japan) with 3,5-dimethoxy-4-hydroxy-cinnamic acid as the matrix.

2.7. *Monosaccharide composition analysis*

Monosaccharide composition analysis was performed according to the method reported by Hardy et al. [23]. Briefly, rhFS (50 µg) was hydrolyzed with 2 M TFA at 100 °C for 3 h. Monosaccharide compositions were analyzed by high-pH anion-exchange chromatography with pulsed amperometric detection (HPAEC-PAD) using a DX-300 system (Dionex, Sunnyvale, CA, USA) equipped with a CarboPac PA-1 anion exchange column (4 × 250 mm, Dionex).

2.8. *Preparation of N-linked oligosaccharides alditols*

N-linked oligosaccharides alditols were prepared by a previously described method [20]. Briefly, rhFS (100 µg) was digested with 5 units of PNGaseF at 37 °C for 2 days. Proteins were precipitated with 75% cold ethanol. The oligosaccharides were incubated with $NaBH_4$ at room temperature for 2 h. Excess reagent was decomposed with diluted acetic acid. The mixture was applied to a Supelclean ENVI-Carb column (Supelco, Bellefonte, PA, USA), which was washed with H_2O to remove the salts. Borohydride-reduced oligosaccharides were eluted with 30% acetonitrile/5 mM ammonium acetate.

2.9. *Sugar profiling by LC/MS*

Sugar profiling was carried out using a MAGIC 2002 system (Michrom BioResources, Inc., Auburn, CA, USA) connected to a TSQ7000 triple-stage quadruple mass spectrometer (ThermoFinnigan, San Jose, CA, USA) in the positive-ion mode. The column used was a GCC (Hypercarb 5 µm, 1.0 × 150 mm, ThermoFinnigan). The eluents were 5 mM ammonium acetate (pH 9.6) containing 2% acetonitrile (pump A); and 5 mM ammonium acetate (pH 9.6) containing 80% acetonitrile (pump B). The N-linked oligosaccharide alditols were eluted at a flow rate of 50 µl/min for 80 min with a gradient of 5–30% in pump B. The ESI voltage was set at 4500 V, and the capillary temperature was 175 °C. The electron multiplier was set at 1200 V.

2.10. *Asp-N digestion*

RhFS was reduced and *S*-carboxymethylated as previously described [20]. Briefly, rhFS (100 µg) was dissolved in 0.5 M Tris–HCl buffer (pH 8.6) containing 8 M guanidine and 5 mM EDTA. After reduction with 2-mercaptoethanol at room temperature for 2 h, mono-iodoacetic acid was added and incubated at room temperature for 2 h in the dark. Reduced and *S*-carboxymethylated-rhFS (equivalent to 100 µg of rhFS) was digested with Asp-N (2 µg) in 25 mM NH_4HCO_3 (pH 8.0) at 37 °C for 20 h. The predicted peptides to be obtained by Asp-N digestion were sequentially designated as D1–D15 (Fig. 1).

2.11. *Peptide/glycopeptide mapping of Asp-N-digested rhFS*

Peptide/glycopeptide mapping was carried out using a MAGIC 2002 system connected to a TSQ7000 triple-stage quadruple mass spectrometer in the positive-ion mode. The column used was a MAGIC C18 column (1.0 × 150 mm, Michrom BioResources). The eluents were 2% acetonitrile/0.05% TFA (pump A), and 80% acetonitrile/0.05% TFA (pump B). Asp-N-digested rhFS was eluted with a linear gradient from 5 to 45% in pump B at a flow rate of 50 µl/min for 40 min. The eluate was monitored at 206 nm. The ESI voltage was set at 4500 V, and the capillary temperature was 175 °C. The electron multiplier was set at 1200 V. Precursor-ion scanning was performed using argon gas as the collision gas at a pressure of 2 mTorr. The collision energy was adjusted to −25 eV. The scan rate was 3 s/scan.

3. Results

3.1. *Heterogeneity of rhFS*

The carbohydrate heterogeneity of rhFS was analyzed by SDS-PAGE with and without PNGaseF digestion. The intact rhFS migrated as bands of an apparent molecular mass of 32 kDa and 33–36 kDa under non-reducing conditions (Fig. 2A, lane 1). PNGaseF digestion resulted in the disappearance of the multiple bands at 33–36 kDa with increases in the 32-kDa band (Fig. 2A, lane 2). These results suggest that the 32 kDa band and higher molecular weight bands are

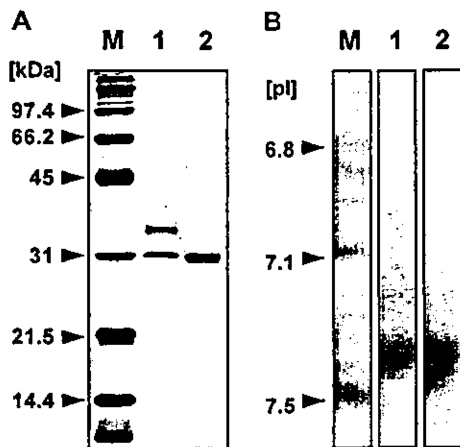

Fig. 2. (A) SDS-PAGE analysis of intact rhFS (lane 1) and PNGaseF-digested rhFS (lane 2). Lane M represents molecular weight markers. (B) IEF of intact rhFS (lane 1) and neuraminidase-digested rhFS (lane 2). Lane M represents p*I* markers.

the non-glycosylated FS and the glycosylated FS with diverse N-linked oligosaccharides, respectively.

The sialic acid heterogeneity of rhFS was analyzed by IEF with and without neuraminidase digestion. IEF of intact rhFS showed that the majority of the isoforms are located from p*I* 6.9 to 7.4 (Fig. 2B, lane 1). After treatment with neuraminidase, the acidic bands had disappeared and shifted at p*I* 7.4 (Fig. 2B, lane 2). These results suggested that the sialic acids contribute to the heterogeneity and the charge of rhFS.

The distribution of glycoforms was further investigated by MALDI-TOF MS. As shown in Fig. 3, multiple ions were detected in the range of 31.5–37 kDa. The most abundant ion at *m/z* 31,525 corresponded to the theoretical mass of non-glycosylated FS (31,514 Da). The other ions at *m/z* 33,804 and 35,600 could have

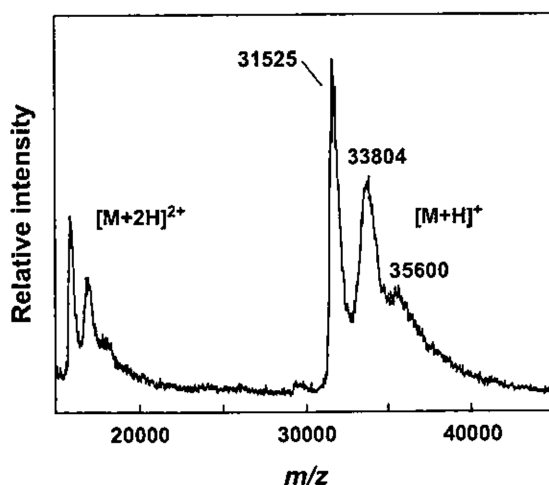

Fig. 3. MALDI-TOF MS analysis of intact rhFS. The peaks at *m/z* 31,525, 33,804 and 35,600 correspond to the non-glycosylated and glycosylated form of rhFS, respectively.

been monoglycosylated FS and diglycosylated FS, respectively.

3.2. Monosaccharide composition of rhFS

Monosaccharide composition was analyzed by hydrolysis followed by HPAEC-PAD. The relative molecular ratio of fucose and glucosamine were estimated at 1.2 and 4.4, respectively, when mannose was considered as 3.0 (Table 1). This result suggests the presence of fucosylated bi- and triantennary-type oligosaccharides. No galactosamine residue was detected, suggesting the absence of O-linked oligosaccharides.

3.3. N-linked oligosaccharides in rhFS

N-linked oligosaccharides were released from rhFS by PNGaseF digestion and reduced with $NaBH_4$ to avoid the separation of anomers. Then the oligosaccharide alditols from rhFS were analyzed by GCC-LC/MS. Fig. 4 shows the total ion current chromatogram of N-linked oligosaccharide alditols. The *m/z* values of intense ions observed in major peaks (peaks 8 and 12) were 1040.7^{2+} and 1186.4^{2+}, which were consistent with the theoretical *m/z* values of $[dHex][Hex]_5[HexNAc]_4[NeuAc]^{2+}$ and $[dHex][Hex]_5[HexNAc]_4[NeuAc]_2{}^{2+}$, respectively (Table 2). The elution times of these oligosaccharides were in good agreement with those of fucosyl biantennary oligosaccharides bearing mono- and di-NeuAc prepared from erythropoietin, respectively [24]. An ion at *m/z* 1041.4^{2+} was also detected in peak 6. This oligosaccharide could be a sialylation isomer of peak 8 (1040.7^{2+}).

Likewise, the ions at *m/z* 1790.7^{+} and 895.4^{2+} in peak 2 and at *m/z* 1077.9^{2+} in peak 3 were assigned as an asialo fucosylated biantennary oligosaccharide and an asialo fucosylated triantennary oligosaccharide, respectively. The ion at *m/z* 2389.6^{+} and 1194.6^{2+} in peak 11 was consistent with $[dHex][Hex]_5[HexNAc]_4[NeuAc][NeuGc]^{2+}$ or $[Hex]_6[HexNAc]_4[NeuAc]_2{}^{2+}$, respectively. The ions at *m/z* 2097.7^{+} and 1048.6^{2+} in peak 5 and at *m/z* 2096.5^{+} and 1049.5^{2+} in peak 8 were consistent with $[dHex][Hex]_5[HexNAc]_4[NeuGc]^{2+}$ or $[Hex]_6[HexNAc]_4[NeuAc]^{2+}$, respectively. The minor ions at *m/z* 1224.1^{2+}, 1224.3^{2+}, 1369.7^{2+}, 1369.8^{2+},

Table 1
Monosaccharide composition analysis of rhFS oligosaccharides

Monosaccharide	Relative molar proportions[a]
Fucose	1.2
Galactosamine	0.3
Glucosamine	4.4
Galactose	3.2
Glucose	0.3
Mannose	3.0

[a] Data are normalized to three-mannose residues.

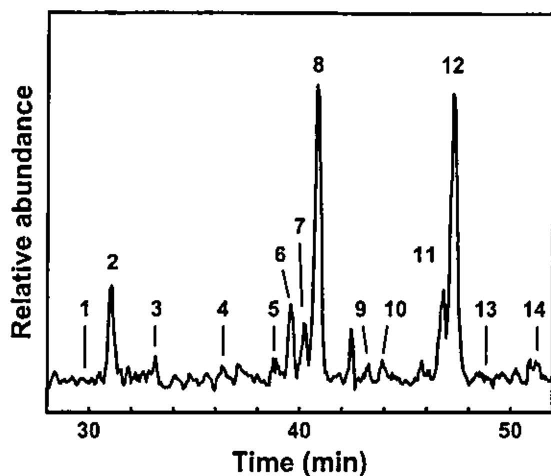

Fig. 4. Sugar map of oligosaccharide alditols released from rhFS. N-linked oligosaccharide alditols from rhFS were separated with GCC. The total ion content was scanned using the positive-ion mode at m/z 700–2400.

1370.5^{2+} and 1515.5^{2+} in peaks 7, 9, 11, 12, 13 and 14 were deduced to the fucosylated triantennary oligosaccharides with NeuAc, respectively.

The ratio of oligosaccharides was estimated as follows: fucosylated biantennary, ca. 85%, and fucosylated triantennary structures, ca. 10%, based on their ion currents; these results were in good agreement with the results of the monosaccharide composition analysis.

3.4. Site-specific glycosylation of rhFS

FS contains two potential N-glycosylation sites (Asn95 and Asn259, Fig. 1). The site-specific glycosylation and other post-translational modifications, such as phosphorylation and hydroxylation, were analyzed by mass spectrometric peptide/glycopeptide mapping (Fig. 5a, Table 3). Most of the non-glycosylated peptides were detected except for the small peptides, i.e. peptides D2 (tripeptide), D13 (tetrapeptide), and D12 (pentapeptide), which suggests the absence of O-glycans and any post-translational modifications on these peptides. The small peptides have no putative N-glycosylation site (Fig. 1), and no galactosamine residue was detected (Table 1). These findings suggest the absence of N- and O-linked oligosaccharides. However, the possibility remains that the small peptides are modified, such as by phosphorylation. Two unpredicted peptides (m/z 1176.2^{2+} and 510.4^{2+}) were detected among the Asp-N digests of rhFS. They were assigned to peptides D15-1 and D15-2, which were produced from peptide D15 by further cleavage at the amino-terminal of Glu280. It was reported that a cleavage at the N-terminal site of glutamic acid is a possible cut site for Asp-N under the same conditions [25]. Peptides D5 and D15-1, each of which have potential glycosylation site, were detected as non-glycosylated forms in the peptide/glycopeptide map.

Table 2
Putative structures of N-linked oligosaccharides deduced from the GCC-LC/MS

Peak No.[a]	Carbohydrate structure[b]	Theoretical mass[c]	Observed mass[d]		
			M^+	M^{2+}	M^{3+}
1		1627.5	1628.3	814.2	-
2		1789.7	1790.7	895.4	-
3		2155.0	-	1077.9	-
4		1934.7	-	967.9	-
5	*1	2096.9	2097.7	1048.6	-
6		2080.9	2081.2	1041.4	-
7		2446.3	-	1224.1	817.4
8	*1	2096.9	2096.5	1049.6	-
		2080.9	2082.2	1040.7	-
9		2446.3	-	1224.3	-
10		2226.0	-	1114.2	-
11	*2	2388.2	2389.6	1194.6	-
		2737.5	-	1369.7	913.4
12		2372.2	2372.2	1186.4	-
		2737.5	-	1369.8	-
13		2737.5	-	1370.5	913.8
14		3028.8	-	1515.5	-

Note: The observed m/z of *1 and *2 are also consistent with the theoretical m/z value of $[Hex]_6[HexNAc]_4[NeuAc]$ and $[Hex]_6[HexNAc]_4[NeuAc]_2$, respectively.
[a] Peak label in Fig. 4.
[b] Proposed structures based on molecular weight. Symbols: solid squares, GlcNAc; open circles, mannose; open diamonds, galactose; dotted diamonds, fucose; solid circle, NeuAc; dotted circle, NeuGc.
[c] Calculated average mass.
[d] Mass of the ion measured in the positive-ion ESI mass spectrum from alditols.

Precursor-ion scanning, which can detect $[Hex][HexNAc]^+$ at m/z 366 produced by collision-induced dissociation, was performed for the monitoring of the glycopeptides. The TIC chromatogram of the precursor-ion scanning showed two significant peaks, peaks G1 and G2 (Fig. 5b). Fig. 6 shows the mass spectra of peaks G1 and G2 in Fig. 5b. On the basis of the theoretical masses of the peptides and oligosaccharides identified by sugar mapping (Table 2), peaks G1 and G2

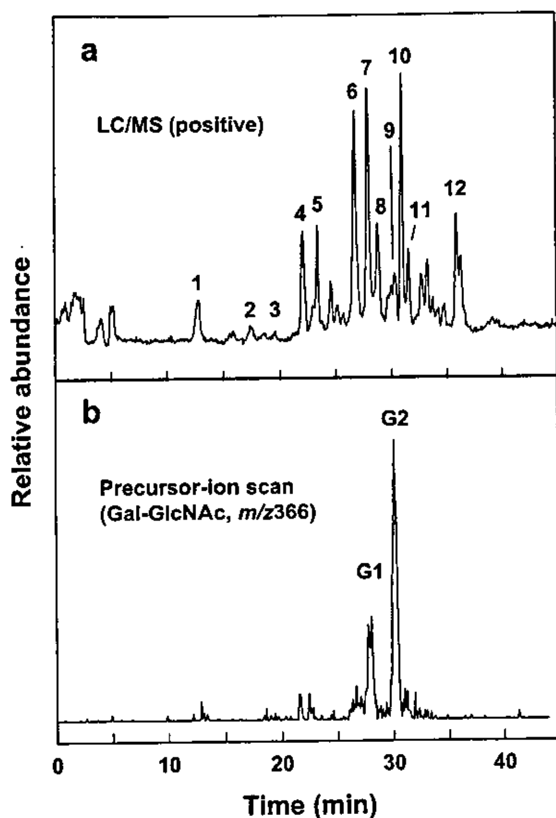

Fig. 5. Peptide/glycopeptide map of the rhFS Asp-N digest. The total ion current chromatogram of LC/MS in the positive-ion mode at m/z 400–2400 (a), and the TIC chromatogram of LC/MS/MS, precursor-ion scan of m/z 366 (b).

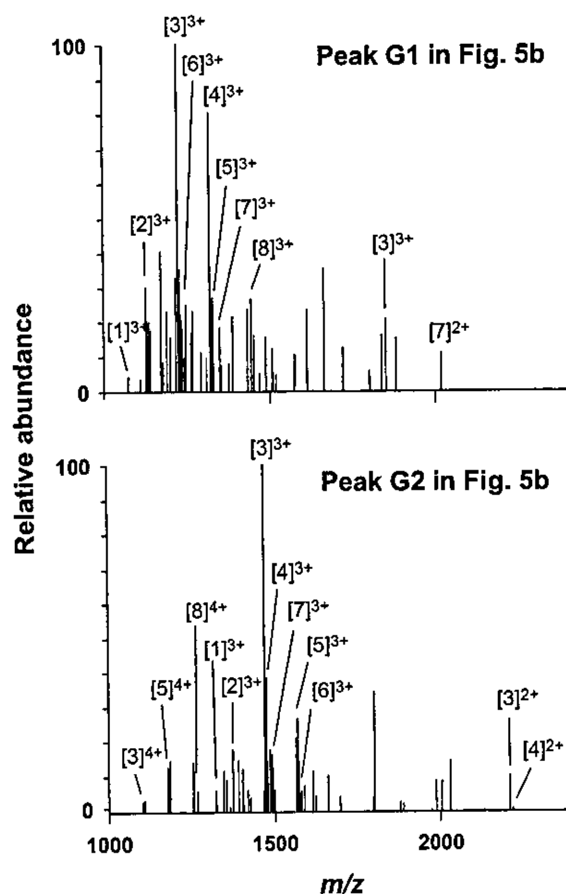

Fig. 6. Mass spectra of glycopeptides in peaks G1 and G2 in Fig. 5b. The observed m/z value of each ion is summarized in Table 4.

were assigned to glycosylated D5 and D15-1, respectively. The oligosaccharides attached to each *N*-glycosylation site were deduced as shown in Table 4. By comparing the N-linked oligosaccharide structures on Asn95 with those on Asn259, it was concluded that biantennary oligosaccharides are major oligosaccharides located at both Asn95 and Asn259, whereas the triantennary structures are present mainly at Asn95.

Table 3
Assignment of the peaks in Fig. 5a

Peak no.[a]	Peptide[b]	Theoretical mass[c]	Observed m/z[d]					
			M^{+}	M^{2+}	M^{3+}	M^{4+}	M^{5+}	M^{6+}
1	D4	2666.0	–	1334.2	889.9	667.4	–	–
2	D14	777.8	778.6	–	–	–	–	–
3	D15-2[e]	1018.0	1019.0	510.4	–	–	–	–
4	D11	1456.6	1457.5	729.0	486.3	–	–	–
5	D6	4378.8	–	–	1460.8	1095.5	–	–
6	D8	3326.4	–	1664.6	1109.5	–	–	–
	D10	1467.6	1468.2	734.8	490.1	–	–	–
7	D1	4728.1	–	–	1577.0	1183.2	947.0	789.6
8	D7	1329.4	1330.2	665.3	–	–	–	–
9	D5	1608.7	1609.3	805.1	–	–	–	–
10	D9	4165.6	–	–	1389.0	1042.2	834.1	–
11	D15-1[e]	2350.6	–	1176.2	784.2	–	–	–
12	D3	3219.5	–	1610.1	1073.8	806.4	–	–

[a] Peak label in Fig. 5a.
[b] Predicted peptides were shown in Fig. 1.
[c] Calculated average mass.
[d] Mass of the ions measured in the positive-ion ESI mass spectrum from precursor-ion scan.
[e] Peptide derived from D15 peptide.

4. Discussion

The aim of the present study was to analyze the distribution of the glycoforms and the carbohydrate structures of rhFS. Previous study of FS isolated from porcine ovary has shown that porcine FS exists in six isoforms, due to alternative splicing and the site occupancy of N-linked oligosaccharides [8]. In this study, we used rhFS288 to eliminate the heterogeneity due to alternative splicing. The results of SDS-PAGE and MALDI-TOF MS revealed the presence of both non-glycosylated and glycosylated forms (Figs. 2 and 3). FS contains two potential *N*-glycosylation sites. Using mass spectrometric peptide/glycopeptide mapping and precursor-ion scanning, we found that both *N*-glycosylation sites were partially glycosylated (Fig. 5 and Table 3). Non-glycosylated and glycosylated proteins containing Asn95 and Asn259 were detected in the peptide/glycopeptide map and precursor-ion scanning, respectively. Monosaccharide composition analyses suggested the presence of linkages of fucosylated bi- and triantennary complex-type oligosaccharides on rhFS (Table 1). This finding was supported by mass spectrometric oligosaccharide profiling, in which the *m/z* values and elution times of some of the oligosaccharides from rhFS were in good agreement with those of standard oligosaccharides. The site-specific glycosylations were deduced on the basis of the mass spectra of glycopeptides. It was suggested that biantennary oligosaccharides attach to both Asn95 and Asn259, whereas triantennary oligosaccharides attach mainly to Asn95 (Fig. 6 and Table 4).

Asn95 is located in the follistatin domain I, which is thought to be the heparin-binding site [26]. The site occupancy and structure of N-linked oligosaccharides on Asn95 may affect the heparin-binding ability of FS. Heparin/heparan sulfate proteoglycans are known to exert an important influence on FS, which neutralizes the activity of activins. It is therefore possible that sialylated oligosaccharides at Asn95 control the activin-neutralizing activity via modulation of the heparin-binding ability of FS. In fact, it was reported that the *N*-glycosylation isoforms of antithrombin and heparin cofactor II differ substantially in their affinity for heparin [27,28]. We are currently studying the role played by oligosaccharides in the activin-neutralizing activity of FS; these studies employ the carbohydrate remodeling technique using the CHO cell line established in the present study.

Table 4
Putative structures of N-linked oligosaccharides deduced from the LC/MS of the glycopeptides corresponding to the Asn95 and Asn259

Carbohydrate Structure[a]	Asn95					Asn259				
	Ions in peak G1	Theoretical mass[b]	Observed m/z [c]			Ions in peak G2	Theoretical mass[b]	Observed m/z		
			M^{2+}	M^{3+}	M^{4+}			M^{2+}	M^{3+}	M^{4+}
	1	3216.2	-	1073.4	-	1	3958.1	-	1319.6	-
	2	3378.6	-	1126.6	-	2	4120.5	-	1373.9	-
	3	3669.6	1835.7	1223.2	-	3	4411.5	2206.3	1471.8	1104.7
	-		-		-	4	4427.5	2214.8	1475.7	-
	4	3960.9	-	1320.6	-	5	4702.8	-	1569.5	1177.1
	5	3976.6	-	1326.8	-	6	4718.8	-	1574.5	-
	6	3743.7	-	1248.6	-	7	4485.6	-	1497.2	-
	7	4034.9	2017.5	1346.9	-	-	-	-	-	-
	8	4326.2	-	1444.1	-	8	5068.1	-	-	1267.6

[a] Proposed structures based on molecular weight. Symbols: solid squares, GlcNAc; open circles, mannose; open diamonds, galactose; dotted diamonds, fucose; solid circle, NeuAc; dotted circle, NeuGc.
[b] Calculated average mass.
[c] Mass of the ion measured in the positive-ion ESI mass spectrum from precursor-ion scan. Mass spectra were shown in Fig. 6.

Acknowledgements

We thank Dr. Y. Eto (Ajinomoto Co., Inc.) for providing the human FS315 cDNA. This work was supported by a grant-in-aid for the Research on Health Sciences Focusing on Drug Innovation from the Japan Health Sciences Foundation.

References

[1] Robertson DM, Klein R, de Vos FL, McLachlan RI, Wettenhall RE, Hearn MT, et al. The isolation of polypeptides with FSH suppressing activity from bovine follicular fluid which are structurally different to inhibin. Biochem Biophys Res Commun 1987;149:744–9.
[2] Ueno N, Ling N, Ying SY, Esch F, Shimasaki S, Guillemin R. Isolation and partial characterization of follistatin: a single-chain Mr 35,000 monomeric protein that inhibits the release of follicle-stimulating hormone. Proc Natl Acad Sci USA 1987;84: 8282–6.
[3] Nakamura T, Takio K, Eto Y, Shibai H, Titani K, Sugino H. Activin-binding protein from rat ovary is follistatin. Science 1990; 247:836–8.
[4] Kogawa K, Nakamura T, Sugino K, Takio K, Titani K, Sugino H. Activin-binding protein is present in pituitary. Endocrinology 1991;128:1434–40.
[5] Massague J. The transforming growth factor-beta family. Annu Rev Cell Biol 1990;6:597–641.
[6] Kingsley DM. The TGF-beta superfamily: new members, new receptors, and new genetic tests of function in different organisms. Genes Dev 1994;8:133–46.
[7] Wada M, Shintani Y, Kosaka M, Sano T, Hizawa K, Saito S. Immunohistochemical localization of activin A and follistatin in human tissues. Endocr J 1996;43:375–85.
[8] Sugino K, Kurosawa N, Nakamura T, Takio K, Shimasaki S, Ling N, et al. Molecular heterogeneity of follistatin, an activin-binding protein. Higher affinity of the carboxyl-terminal truncated forms for heparan sulfate proteoglycans on the ovarian granulosa cell. J Biol Chem 1993;268:15579–87.
[9] Patel K. Follistatin. Int J Biochem Cell Biol 1998;30:1087–93.
[10] Inouye S, Guo Y, DePaolo L, Shimonaka M, Ling N, Shimasaki S. Recombinant expression of human follistatin with 315 and 288 amino acids: chemical and biological comparison with native porcine follistatin. Endocrinology 1991;129:815–22.
[11] Sumitomo S, Inouye S, Liu XJ, Ling N, Shimasaki S. The heparin binding site of follistatin is involved in its interaction with activin. Biochem Biophys Res Commun 1995;208:1–9.
[12] Hashimoto O, Nakamura T, Shoji H, Shimasaki S, Hayashi Y, Sugino H. A novel role of follistatin, an activin-binding protein, in the inhibition of activin action in rat pituitary cells. Endocytotic degradation of activin and its acceleration by follistatin associated with cell-surface heparan sulfate. J Biol Chem 1997;272: 13835–42.
[13] Kobata A. Structures and functions of the sugar chains of glycoproteins. Eur J Biochem 1992;209:483–501.
[14] Varki A. Biological roles of oligosaccharides: all of the theories are correct. Glycobiology 1993;3:97–130.
[15] Itoh S, Kawasaki N, Ohta M, Hyuga M, Hyuga S, Hayakawa T. Study on evaluating methods for the quality control of glycoprotein products. (III)—Erythropoietin products. Part 3. Bull Natl Inst Health Sci 2001;65–9.
[16] Simultaneous microanalysis of N-linked oligosaccharides in a glycoprotein using microbore graphitized carbon column liquid chromatography—mass spectrometry. J Chromatogr A 2002;968: 89–100.
[17] Kawasaki N, Ohta M, Hyuga S, Hashimoto O, Hayakawa T. Analysis of carbohydrate heterogeneity in a glycoprotein using liquid chromatography/mass spectrometry and liquid chromatography with tandem mass spectrometry. Anal Biochem 1999;269: 297–303.
[18] Kawasaki N, Ohta M, Hyuga S, Hyuga M, Hayakawa T. Application of liquid chromatography/mass spectrometry and liquid chromatography with tandem mass spectrometry to the analysis of the site-specific carbohydrate heterogeneity in erythropoietin. Anal Biochem 2000;285:82–91.
[19] Kawasaki N, Haishima Y, Ohta M, Itoh S, Hyuga M, Hyuga S, et al. Structural analysis of sulfated N-linked oligosaccharides in erythropoietin. Glycobiology 2001;11:1043–9.
[20] Kawasaki N, Ohta M, Itoh S, Hyuga M, Hyuga S, Hayakawa T. Usefulness of sugar mapping by liquid chromatography/mass spectrometry in comparability assessments of glycoprotein products. Biologicals 2002;30:113–23.
[21] Ohta M, Kawasaki N, Hyuga S, Hyuga M, Hayakawa T. Selective glycopeptide mapping of erythropoietin by on-line high-performance liquid chromatography—electrospray ionization mass spectrometry. J Chromatogr A 2001;910:1–11.
[22] Ohta M, Kawasaki N, Itoh S, Hayakawa T. Usefulness of glycopeptide mapping by liquid chromatography/mass spectrometry in comparability assessment of glycoprotein products. Biologicals 2002;30:235–44.
[23] Hardy MR, Townsend RR, Lee YC. Monosaccharide analysis of glycoconjugates by anion exchange chromatography with pulsed amperometric detection. Anal Biochem 1988;170:54–62.
[24] Kawasaki N, Ohta M, Hyuga S, Hyuga M, Hayakawa T. Application of liquid chromatography/mass spectrometry and liquid chromatography with tandem mass spectrometry to the analysis of the site-specific carbohydrate heterogeneity in erythropoietin. Anal Biochem 2000;285:82–91.
[25] Ingrosso D, Fowler AV, Bleibaum J, Clarke S. Specificity of endoproteinase Asp-N (Pseudomonas fragi): cleavage at glutamyl residues in two proteins. Biochem Biophys Res Commun 1989; 162:1528–34.
[26] Inouye S, Ling N, Shimasaki S. Localization of the heparin binding site of follistatin. Mol Cell Endocrinol 1992;90:1–6.
[27] Picard V, Ersdal-Badju E, Bock SC. Partial glycosylation of antithrombin III asparagine-135 is caused by the serine in the third position of its *N*-glycosylation consensus sequence and is responsible for production of the beta-antithrombin III isoform with enhanced heparin affinity. Biochemistry 1995;34:8433–40.
[28] Bohme C, Nimtz M, Grabenhorst E, Conradt HS, Strathmann A, Ragg H. Tyrosine sulfation and *N*-glycosylation of human heparin cofactor II from plasma and recombinant Chinese hamster ovary cells and their effects on heparin binding. Eur J Biochem 2002;269:977–88.

Enhancement of Hepatocyte Growth Factor-Induced Cell Scattering in *N*-Acetylglucosaminyltransferase III-transfected HepG2 Cells

Masashi HYUGA,* Sumiko HYUGA, Nana KAWASAKI, Miyako OHTA, Satsuki ITOH, Shingo NIIMI, Toru KAWANISHI, and Takao HAYAKAWA

Division of Biological Chemistry and Biologicals, National Institute of Health Sciences; 1–18–1 Kamiyoga, Setagaya-ku, Tokyo 158–8501, Japan. Received January 9, 2004; accepted March 29, 2004; published online April 1, 2004

N-Acetylglucosaminyltransferase III (GnT-III), which catalyzes the synthesis of a bisecting GlcNAc residue of N-glycans, is thought to be involved in the function of glycoproteins such as growth factor receptors. We investigated the effects of the overexpression of GnT-III on the hepatocyte growth factor (HGF) receptor c-Met, a glycoprotein, in human hepatocarcinoma HepG2 cells. GnT-III activity was elevated about 250-fold in HepG2 cells stably transfected with the GnT-III gene, whereas no significant change in GnT-III activity was observed in mock transfectants. Cell scattering assay revealed that HGF-induced cell scattering was enhanced depending on the GnT-III activities in the GnT-III transfectants. Western blot analysis and E-PHA lectin blot analysis showed that the level of c-Met protein was the same in both transfectants; however, the bisecting GlcNAc residue on c-Met was detected only in the GnT-III transfectants. Although the peak level of c-Met phosphorylation was not different in both transfectants, the level of tyrosine phosphorylation of c-Met decreased more rapidly in the GnT-III transfectants than in the mock transfectants. Furthermore, HGF-induced extracellular-regulated kinase (ERK) phosphorylation was slightly higher in the GnT-III transfectants than in the mock transfectants. These results show that overexpression of GnT-III in HepG2 cells enhances HGF-induced cell scattering, which may result from, at least in part, enhancement of HGF-induced ERK phosphorylation.

Key words *N*-acetylglucosaminyltransferase III; cell scattering; hepatocyte growth factor; c-Met; extracellular-regulated kinase (ERK)

N-Acetylglucosaminyltransferase III (GnT-III: EC 2.4.1.144) is one of the glycosyltranferases and catalyzes the synthesis of a bisecting GlcNAc residue to the β-mannoside of the trimannose core in *N*-glycans.[1] After introduction of the bisecting GlcNAc residue to the biantennary sugar chain, further processing and elongation of *N*-glycans by the other glycosyltransferases are suppressed,[2—4] resulting in alterations of structure with reduction of size. It seems that GnT-III may affect the functions of various glycoproteins. In this respect, it is noteworthy that the overexpression of GnT-III affects receptor tyrosine kinases such as the epidermal growth factor (EGF) and NGF receptor Trk, followed by the modulation of signal transductions.[5] EGF inhibits the growth of U373 MG glioma cells, while the overexpression of GnT-III causes the decreased binding of EGF to its receptor and then autophosphorylation of the receptor, resulting in the increase in the cell growth rate.[6] In contrast, the overexpression of GnT-III in HeLaS3 cells does not affect EGF receptor autophosphorylation, but enhances internalization of the receptors, resulting in the increase of the EGF-induced phosphorylation of extracellular-regulated kinase (ERK).[7] In PC 12 cells, nerve growth factor-stimulated Trk receptor autophosphorylation and signal transduction was disrupted by the overexpression of GnT-III.[8] This evidence suggests that GnT-III may also affect the other growth factors-induced signal transduction by the modulation of the function of their receptors in some ways.

Since the expression of GnT-III is associated with many physiological and pathological processes in the liver, including its regeneration[9] and hepatocarcinogenesis,[10] it is assumed that GnT-III is involved in the processes via the modulation of some glycoproteins such as the receptor of the hepatocyte growth factor (HGF), c-Met. In the present study, we investigated the effects of the overexpression of GnT-III on the scattering of human hepatocarcinoma HepG2 cells, a defined HGF-induced biological response.

MATERIALS AND METHODS

Materials The recombinant human HGF was purchased from R&D systems (Minneapolis, MN, U.S.A.). The Dulbecco's modified Eagle's medium (DMEM), fetal calf serum (FCS), ampicillin, G418, Lipofectamine plus, and Opti-MEM were purchased from Life Technologies Inc. (Rockville, MD, U.S.A.). The human brain cDNA was purchased from Origene Technologies Inc. (Rockville, MD, U.S.A.). The mammalian expression vector pCI-neo was purchased from Promega (Madison, WI, U.S.A.). The protease inhibitors cocktail was purchased from Sigma Chemical Co (St. Louis, MO, U.S.A.). The PVDF membrane was purchased from Millipore Corporation (Bedford, MA, U.S.A.). Biotinylated E-PHA was purchased from Vector Laboratories (Burlingame, CA, U.S.A.). Protein G-immobilized magnetic beads (BioMag Protein G) were purchased from Polysciences, Inc. (Warrington, PA, U.S.A.). The anti-human c-Met antibody (C-23), anti-phospho-ERK antibody (E-4) and anti-ERK antibody (K-23) were purchased from Santa Cruz Biotechnology, Inc. (Santa Cruz, CA, U.S.A.). The monoclonal anti-phosphotyrosine antibody (PY20) was purchased from Transduction Laboratories (Lexington, KY, U.S.A.). The biotinylated anti-mouse IgG antibody, biotinylated anti-rabbit IgG antibody, peroxidase-conjugated rabbit anti-mouse IgG, and ECL chemiluminescence detection kit were purchased from Amersham-Pharmacia Biotech (Piscataway, NJ, U.S.A.). The vectastain ABC kit was purchased from Vector Laboratories (Burlingame, CA, U.S.A.). All other chemicals were obtained from commercial sources, and were of the highest purity available.

* To whom correspondence should be addressed. e-mail: mhyuga@nihs.go.jp
© 2004 Pharmaceutical Society of Japan